Ain Shams Engineering Journal (2016) xxx, xxx–xxx

Ain Shams University

Ain Shams Engineering Journal

www.elsevier.com/locate/asej
www.sciencedirect.com

ELECTRICAL ENGINEERING

Adaptive chemical reaction based spatial fuzzy clustering for level set segmentation of medical images

V. Asanambigai, J. Sasikala *

Department of Computer Science and Engineering, Annamalai University, Tamil Nadu, India

Received 5 June 2016; revised 27 July 2016; accepted 6 August 2016

KEYWORDS

Segmentation;
Chemical reaction optimization;
Fuzzy c-means;
Level set evolutions

Abstract The chemical reaction optimization (CRO), inspired from the interactions of molecules during chemical reactions in reaching a low energy stable state, searches for optimal solution through simulated reactions involving the on-wall ineffective collisions, decomposition, intermolecular ineffective collision and synthesis. This paper attempts to obtain the global best centroids for spatial fuzzy clustering (SFC) using adaptive CRO (ACRO) with a view to facilitate the level set segmentation for medical images. The approach helps to analyze tumors or unhealthy region in various medical images. The results of medical images of brain, liver, abdomen and eye images are presented to demonstrate the performance.

1. Introduction

Cancer has been one of the biggest threats to human life for the past few decades. It is expected to become the leading cause of death over the next few decades. Based on the statistics from the World Health Organization (WHO), cancer accounted for 7.6 million deaths which are around 13% of all deaths worldwide in the year 2011. Deaths caused by cancer are projected to increase in the future, with an estimated 11 million people dying from cancer in the year 2030 [1]. As the survival rate of the cancer patients detected at later stages is very low, early detection of cancer is very important to cure the fatal disease. Image segmentation is one of the most difficult and challenging tasks in medical image analysis, which endeavors to divide an image into several non-overlapping meaningful regions with homogeneous characteristics in respect of texture, gray value, position, etc., [2] and helps the radiologist to segment the portion of tumor or unhealthy part of the medical images.

Chemical reaction optimization (CRO), a population based stochastic optimization technique inspired from the process of chemical reactions, has been recently suggested for solving combinatorial optimization problems by Lam et al. [3,4]. The CRO has been applied to a variety of real world optimization problems [5–7] and found to yield satisfactory results, and to date, it has not been applied to image segmentation. This paper aimed to apply CRO in segmenting medical images.

As most of the existing segmentation methods are problem specific, which are tailored for any one specific type of images

* Corresponding author.
E-mail address: sasikala_07@rediffmail.com (J. Sasikala).
Peer review under responsibility of Ain Shams University.

Production and hosting by Elsevier

http://dx.doi.org/10.1016/j.asej.2016.08.003

Please cite this article in press as: Asanambigai V, Sasikala J, Adaptive chemical reaction based spatial fuzzy clustering for level set segmentation of medical images, Ain Shams Eng J (2016), http://dx.doi.org/10.1016/j.asej.2016.08.003

Nomenclature

ACRO	adaptive chemical reaction optimization
buffer	central energy buffer
CRO	chemical reaction optimization
C	number of clusters
DiceCo	Dice coefficients
FCM	fuzzy C-means
FP	False Positive
FN	False Negative
IFCM	intuitionistic fuzzy C-means
JacInd	Jaccard index
KM	K-means
KE	kinetic energy
KE_i	kinetic energy of molecule-i
LR	loss rate, indicating percentage upper limit of reduction of KE in on-wall ineffective collisions
l	a parameter (>1) controlling the fuzziness of the segmentation
N_n	a local window centered around the image pixel n
n	number of decision variables
PM	proposed method
PE	potential energy
PS	population size
p	a random number in the range of [0, 1]
PE_i	potential energy of molecule-i
q	a random number in the range of [LR, 1]
R_k	a contour of interest in FCM results of μ
SFC	spatial fuzzy clustering
TP	True Positive
TN	True Negative
TH	thresholding
$t_{\max}$	maximum number of iterations
x	vector of dependant variables
u	vector of control or independent variables
v	the customable balloon force
w	weight constant
molecoll	fraction of all elementary reactions corresponding to intermolecular reactions
ω_i	structure of i-th molecule
$\Delta\omega_i$	perturbations to structure of i-th molecule
Δ	fixed interval
σ	the step size
θ	decrement constant
α	a parameter that decides the type of uni-molecular reaction
β	minimum kinetic energy of a molecule
μ_{mn}	membership of the n-th object to the m-th cluster
ε	a constant regulating the Dirac function
b_0	an adjustable threshold in the range of (0, 1)
∇	operation for an image gradient
$\lvert\nabla\phi\rvert$	the normal direction
η	penalty coefficient
%*SenInd*	percentage sensitivity index
%*SpeInd*	percentage specificity index
Θ_{GT}	manually segmented ground truth region
Θ_{CM}	area detected by the computerized method
superscript min and max	lower and upper limits respectively
superscript $'$	respective new/updated value

such as brain or liver or a particular part of the human body, and the radiologist requires an interactive computer aided tool to segment the portion of cancer or diseased parts in medical images belonging to various parts of the body, this paper suggests an adaptive CRO (ACRO) based interactive segmentation tool involving level set evolutions for detecting unhealthy part in medical images with a view of decreasing the possibility of falling the cluster centers into local minima and considering the spatial information. The results on various medical images are presented to demonstrate the effectiveness of the developed strategy. The paper is divided into six sections. Section 1 presents the introduction, Section 2 reviews the related work, Section 3 explains ACRO, Section 4 proposes the new segmentation method comprising ACRO based SFC and level set evolutions, Section 5 discusses the results and Section 6 concludes.

2. Related work

Numerous segmentation methods have been suggested in the recent decades. These methods can be classified into three categories: threshold-based, deformation-based and clustering-based. The threshold-based methods determine threshold values using the image histogram and then classify the image pixels based on these values [8–11]; deformation-based methods, employing region growing [12,13] and level set [14,15] approaches, have been proposed for identification of the cancer boundary. Most of the deformation-based segmentation methods are semiautomatic since the generation of initial points is difficult to automate. The region growing methods group the pixels into homogeneous regions and segment the image into some major areas, while the level set methods utilize dynamic variational boundaries for segmentation; The clustering-based methods segment the feature space of image into several clusters and derive a sketch of the original image, such as K-means [16–18], Fuzzy C-means (FCM) [19–22] and mean-shift [23] algorithms. As the crisp segmentation methods restrict each pixel exclusively to one class, they cannot be fruitfully applied to medical images, wherein each pixel does not belong to a particular class. The fuzzy clustering algorithms can assign one pixel to several classes concurrently and keep information as much as possible, thereby making them suitable for medical image segmentation. But most of them includes many small regions in the segmented results due to issues like small scale of spatial resolution, poor illumination, presence of noise and intensity imbrications.

Swarm intelligence based optimization techniques have been applied in solving optimization problem in many science and engineering domains in recent years. A dynamic clustering approach based on particle swarm optimization (PSO) that determines optimum number of centroids for image segmenta-

Please cite this article in press as: Asanambigai V, Sasikala J, Adaptive chemical reaction based spatial fuzzy clustering for level set segmentation of medical images, Ain Shams Eng J (2016), http://dx.doi.org/10.1016/j.asej.2016.08.003

tion has been suggested in [24]. A fast image segmentation method based on artificial bee colony (ABC) optimization to estimate the appropriate threshold values in a continuous gray scale interval has been outlined in [25]. A hybrid approach of matched filter and ant colony optimization for extraction of blood vessels in ophthalmoscope images has been presented in [26]. A color clustering method based on ant colony optimization for the detection of flower boundaries has been notified in [27]. The search abilities of PSO and ABC have been exploited in multi-level thresholding in [28]. The cuckoo search algorithm has been applied in determining optimal coefficients of a fractional delay-infinite impulse response filter with a view of meeting the ideal frequency response characteristics in [29,30]. A real coded genetic algorithm based optimal design of linear phase digital finite impulse response band stop filter using the L1-norm has been outlined in [31]. A semi-supervised clustering technique using the concepts of multi objective optimization has been suggested for automatic segmentation of MR brain images in the intensity space in [32]. A PSO based image segmentation strategy with modified learning operators for enhancing the exploration ability and convergence has been outlined in [33].

3. Adaptive CRO

In chemical reactions, the molecules of initial reactants possessing high-energy unstable states, undergo a sequence of collisions either with walls of the container or with other molecules, pass through some energy barriers and become final products by releasing energy. The final products generally have less energy, thereby making them more stable than the reactants. This phenomenon of driving the molecules from high-energy unstable states to low-energy stable states by chemical reaction can be related to the process of minimizing the objective function value in optimization problems through adjusting the control variables. Inspired from this relation, CRO algorithm for solving multimodal optimization problems has been developed by Lam et al. [3,4]. The CRO algorithm involving the prime components of the chemical reactions (i.e., molecules and elementary reactions) is narrated below.

3.1. Molecules

The manipulated agents are molecules, each composing of several atoms. One molecule is distinct from another when they contain different atoms and/or different number of atoms and characterized by its structure (ω). Each ω denotes a solution point in the problem space and can be represented in vector form as

$$\omega_i = [\omega_i(1), \omega_i(2), \ldots, \omega_i(n)] \tag{1}$$

where $\omega_i(j)$ represents j-th control variable of i-th molecular structure, lying within the respective lower and upper bounds.

A molecule possesses two kinds of energies, the potential energy (PE) and the kinetic energy (KE). The former quantifies the molecular structure in terms of energy, while the latter represents a measure of tolerance for the molecule changing to a less favorable structure. Each molecule therefore contains a profile of several properties such as ω, PE and KE. The PE represents the problem objective function for each solution point ω as

$$\text{Minimize } PE_i = f(\omega_i) \tag{2}$$

When the algorithm evolves, the molecules adjust their structure to possess lower PE and KE and the removed energy is stored in a central energy buffer (*buffer*).

3.2. Elementary reactions

In a chemical reaction process, a sequence of collisions among molecules occurs. Molecules collide either with each other or with the walls of the container, resulting in an internal change of molecules. There are four types of elementary reactions implemented in CRO, namely, on-wall ineffective collision, decomposition, inter-molecular ineffective collision, and synthesis. These reactions explore the solution space in search of optimal solution.

On-wall ineffective collision: An on-wall ineffective collision, which is not vigorous, takes place when a molecule-i hits a wall of the container and then bounces back with a small change to its molecular structure as

$$\omega_i'(j) = \omega_i(j) + \Delta\omega_i(j) \tag{3}$$

where $\Delta\omega_i(j)$ represents the perturbations to $\omega_i(j)$.

The newly generated molecular structure ω_i' is in the neighborhood of ω_i and accepted, if the following condition is satisfied:

$$PE_i + KE_i \geqslant PE_i' \tag{4}$$

In light of the fact that the energy can be neither created nor destroyed, KE cannot be intentionally added or removed from a molecule. Since this reaction involves an interaction with the wall of the container, a certain portion of its KE will be extracted and stored in the *buffer*. The size of KE loss depends on a random number $q \in [LR, 1]$. The KE and *buffer* are updated as

$$KE_i' = (PE_i - PE_i' + KE_i) \times q \tag{5}$$

$$buffer' = buffer + (PE_i - PE_i' + KE_i) \times (1 - q) \tag{6}$$

If Eq. (4) does not hold, the change is prohibited and the molecule retains its original ω_i, PE_i and KE_i.

Decomposition: In this reaction, a molecule ω_i hits the wall of the container vigorously and then breaks into two molecules ω_j' and ω_k', which are generated by adding small perturbations to $n/2$ randomly chosen variables of the original ω_i. The new molecular structures are accepted when the following is satisfied:

$$PE_i + KE_i \geqslant PE_j' + PE_k' \tag{7}$$

If Eq. (7) holds, the KE of both molecules are updated as

$$KE_j' = KE_{net} \times p \tag{8}$$

$$KE_k' = KE_{net} \times (1 - p) \tag{9}$$

where $KE_{net} = PE_i + KE_i - PE_j' - PE_k'$ and p is a random number generated in the range (0, 1).

Eq. (7) holds only when KE_i is large enough. However, KE of molecules tends to decrease as the chemical process evolves. Thus, Eq. (7) may not hold in later stages of the reaction process. The energy stored in the *buffer* is utilized to sustain PE_j' and PE_k' with a view to encourage the decomposition. In other words, if Eq. (7) does not hold, the new molecular structures are accepted based on the following criteria:

Please cite this article in press as: Asanambigai V, Sasikala J, Adaptive chemical reaction based spatial fuzzy clustering for level set segmentation of medical images, Ain Shams Eng J (2016), http://dx.doi.org/10.1016/j.asej.2016.08.003

$$PE_i + KE_i + buffer \geqslant PE'_j + PE'_k \quad (10)$$

If Eq. (10) holds, the KE and $buffer$ are updated as

$$KE'_j = (KE_{net} + buffer) \times m_1 \times m_2 \quad (11)$$

$$KE'_k = (KE_{net} + buffer - KE'_j) \times m_3 \times m_4 \quad (12)$$

$$buffer' = buffer + (KE_{net} - KE'_j - KE'_k) \quad (13)$$

where m_1, m_2, m_3 and m_4 are random numbers independently generated in the interval (0, 1).

If both Eqs. (7) and (10) do not hold, the decomposition fails and the molecule retains its original ω_i, PE_i and KE_i. Unlike on wall ineffective collision making local search, the decomposition explores the other regions corresponding to ω'_j and ω'_k.

Inter-molecular ineffective collision: This reaction describes the situation when two molecules collide with each other and then bounce away similar to on-wall ineffective collision. The new molecular structures ω'_i and ω'_j are obtained from their own neighborhoods of ω_i and ω_j separately. The new molecules are accepted only if

$$PE_i + PE_j + KE_i + KE_j \geqslant PE'_i + PE'_j \quad (14)$$

If Eq. (14) holds, the KE of both molecules are updated as

$$KE'_i = KE_{sum} \times p \quad (15)$$

$$KE'_j = KE_{sum} \times (1 - p) \quad (16)$$

where $KE_{sum} = PE_i + PE_j + KE_i + KE_j - PE'_i - PE'_j$ and p is a random number generated in the range (0, 1). The molecules maintain the original $\omega_i, \omega_j, PE_i, PE_j, KE_i$ and KE_j if Eq. (14) fails.

Synthesis: This reaction depicts a situation when two molecules vigorously collide and combine together. The new molecular structure ω'_k is different from the original molecules ω_i and ω_j. Each component of ω'_k is probabilistically selected either from ω_i or from ω_j as explained in [4]. The new structure is accepted by the following criterion:

$$PE_i + PE_j + KE_i + KE_j \geqslant PE'_k \quad (17)$$

If Eq. (17) holds, the new molecular structure ω' is accepted and its KE is updated by

$$KE'_k = PE_i + PE_j + KE_i + KE_j - PE'_k \quad (18)$$

Else, the original solutions ω_i and ω_j are retained without any change.

Adaptive adjustment: The $\Delta\omega_i(j)$, the perturbations to $\omega_i(j)$, is obtained by Gaussian distribution, whose probability density function is given by

$$f_{pdf}(x) = \frac{1}{\sqrt{2\pi\sigma^2}} e^{\left(\frac{-x^2}{2\sigma^2}\right)} \quad (19)$$

where σ is the step size that influences how wide Eq. (20) spreads around zero. If σ is chosen to be too large for a particular problem, the algorithm may not investigate each region thoroughly, fail to locate the minimum of the region, and jump to other regions rashly. If σ is too small, the algorithm will become highly inefficient. The success of any algorithm in obtaining a good solution to a problem will be higher if the algorithm adaptively adjusts its parameters to fit the problem. The adaptive scheme, suggested in [28] decreases the step size through a factor θ at fixed interval Δ by the following equation:

$$\sigma = \sigma \times \theta \quad (20)$$

This scheme ensures that the algorithm will not be too inefficient and too randomized to shuttle around the search space. The additional parameters, θ and Δ, are generally fixed for all problems while σ needs to be tuned for different problems.

Solution process: The values of various CRO parameters, $PS, molecoll, LR, buffer, KE^0, \sigma, \alpha$ and β are chosen. An initial molecule set with size equal to PS is then randomly generated in the solution space. Their initial PEs are determined by their corresponding objective function values while their initial KEs are set to KE^0. In each iteration, there is one elementary reaction taking place. A random number $b \in [0, 1]$ is generated and compared with $molecoll$ to determine whether the reaction is unimolecular or intermolecular reaction happens.

For each unimolecular reaction, one molecule is randomly chosen and a check is made whether it satisfies the decomposition criterion: (number of hits − minimum hit number) > α, where α is the tolerance of duration for the molecule without obtaining any new local minimum solution. If so, the molecule will experience a decomposition, else it will take an on-wall ineffective collision. The molecule with lowest PE is recorded and the iterative process is continued until any one of the stopping criterion is met. After convergence, the molecule with the lowest PE is considered as the optimal solution. A stopping criterion may be defined based on the maximum amount of CPU time used, the maximum number of iterations performed, an objective function value less than a predefined threshold obtained, the maximum number of iterations performed without improvements or any other appropriate criteria.

For each intermolecular reaction, two molecules are selected and tested against the synthesis criterion: $(KE \leqslant \beta)$, where β is the minimum KE a molecule should have. If it is satisfied by the selected molecules, they combine through synthesis. Otherwise, they experience an intermolecular ineffective collision.

During iterations, the number of solutions in the population (PS) may change, as the decomposition and synthesis increase and decrease the number of molecules in the container, respectively - decomposition breaks a molecule into two or more, whereas synthesis combines two or more molecules into one. The detailed pseudo code is available in [3].

4. Proposed method

The proposed ACRO based SFC method (PM) involves ACRO based SFC and adaptive level set evolutions. It begins with ACRO based SFC, which determines the approximate contours of interest in a medical image and its results are utilized to adaptively adjust control parameters and refine segmentation by level set evolutions. This section describes the PM.

4.1. ACRO based SFC

In fuzzy clustering, the centroid and the scope of each subclass are estimated adaptively through an iterative process with a view to minimize the predefined cost function. The spatial information can also be incorporated in the membership func-

tion in order to eliminate intermediate morphological operations. The PM attempts to minimize the *PE* function through estimating the centroids. The cost function of SFC algorithm is considered as the *PE* function, which utilizes a membership function μ_{mn} possessing spatial information:

$$\text{Minimize } PE = \sum_{m=1}^{C}\sum_{n=1}^{N}\mu_{mn}^{l}\|i_n - v_m\|^2 \tag{21}$$

where

$$\mu_{mn} = \frac{a_{mn}^{p} h_{mn}^{q}}{\sum_{k=1}^{C} a_{kn}^{p} h_{kn}^{q}} \tag{22}$$

$$a_{mn} = \frac{\|i_n - v_m\|^{-2/(l-1)}}{\sum_{k=1}^{C}\|i_n - v_k\|^{-2/(l-1)}} \tag{23}$$

$$h_{mn} = \sum_{k\in N_n} a_{mk} \tag{24}$$

In PM, the *PE* function is minimized through controlling the centroids. Each molecular structure-ω_i is defined to denote the decision variables of the centroids in vector form as

$$\omega_i = [v_1, v_2, \ldots, v_C] \tag{25}$$

The perturbations $\Delta\omega$, added to ω_i, may sometimes take a molecule out of the boundaries. The hybrid scheme suggested in [4] combining the absorbing and reflecting principles is used to handle the boundary constraints in the proposed formulation as narrated below:

$$\omega_i'(j) = \begin{cases} LB(j) & \text{if } (\gamma \leqslant 0.5) \text{ AND } (\omega(j) < LB(j)) \\ UB(j) & \text{if } (\gamma \leqslant 0.5) \text{ AND } (\omega(j) > UB(j)) \\ 2 * LB(j) - \omega(j) & \text{if } (\gamma > 0.5) \text{ AND } (\omega(j) < LB(j)) \\ 2 * UB(j) - \omega(j) & \text{if } (\gamma > 0.5) \text{ AND } (\omega(j) > UB(j)) \end{cases} \tag{26}$$

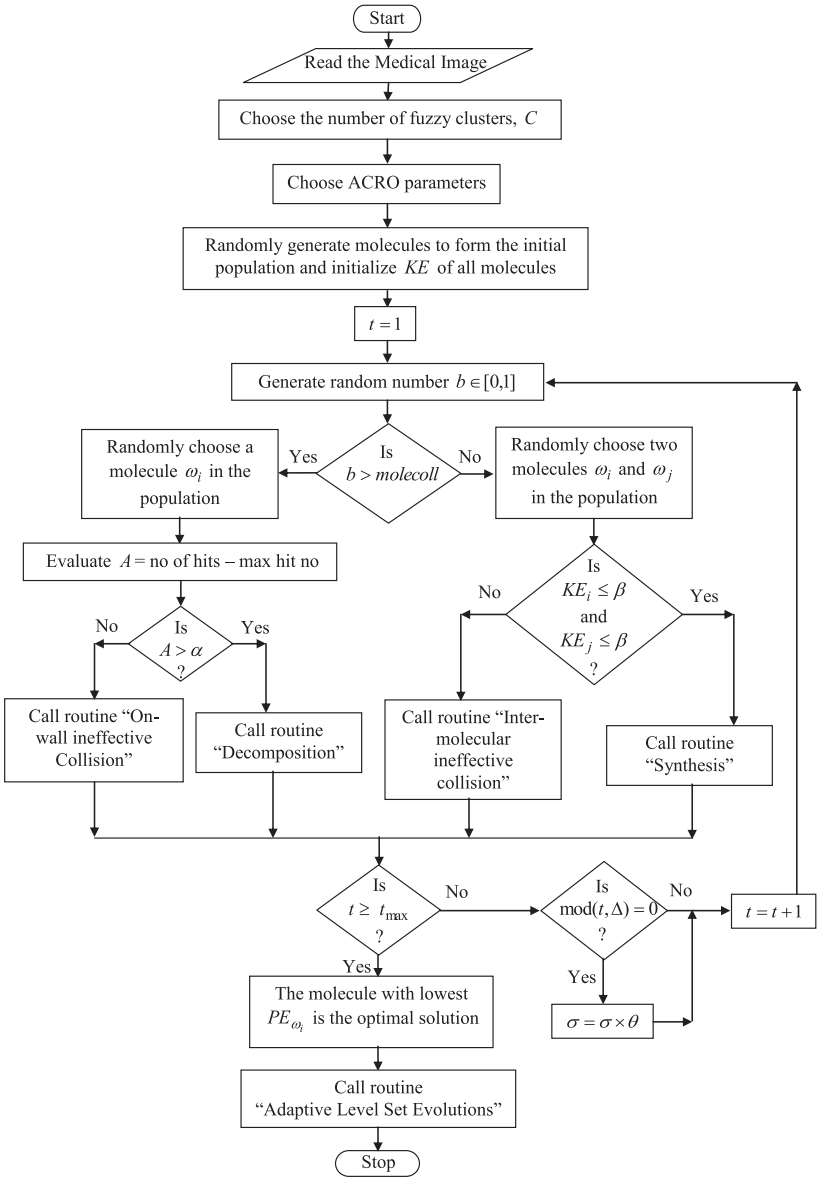

Figure 1 Flowchart of the PM.

where γ is a random number in the range [0, 1]. $LB(j)$ and $UB(j)$ are the respective lower and upper limits for j-th decision variable.

4.2. Adaptive level set evolutions

The membership functions μ of ACRO based SFC represent the approximately segmented contours. Suppose the contour of interest is $R_k : r_k = \mu_{nk}, \{n = x \times N_y + y\}$, the level set function is then initiated by

$$\phi_0(x, y) = -4\varepsilon(0.5 - B_k) \tag{27}$$

where $B_k = R_k \geqslant b_0$

The final contour is obtained through level set evolution by

$$\phi^{k+1}(x, y) = \phi^k(x, y) + \tau[\eta\zeta(\phi^k) + \xi(g, \phi^k)] \tag{28}$$

where $\zeta(\phi^k) = \Delta\phi - div\left(\frac{\nabla\phi}{|\nabla\phi|}\right)$, represents a penalty momentum of ϕ, deviating from the signed distance function. It forces ϕ to approach the genuine signed distance function.

$\xi(g, \phi^k) = \lambda\delta(\phi)div\left(g\frac{\nabla\phi}{|\nabla\phi|}\right) + vg\delta(\phi)$, incorporates image gradient information, which attracts ϕ toward the variational boundary.

$\delta(\phi) = \begin{cases} 0 & |\phi| > \varepsilon \\ \frac{1}{2\varepsilon}\left[1 + \cos\left(\frac{\pi\phi}{\varepsilon}\right)\right] & |\phi| \leqslant \varepsilon \end{cases}$, denotes the Dirac function.

$g = \frac{1}{1+|\nabla(G_\sigma * I)|^2}$, represents edge indication function.

$G_\sigma * I$ stands for the convolution of the image I with a smoothing Gaussian kernel G_σ.

The segmentation process during evolution of Eq. (27) requires appropriate selection of several control parameters

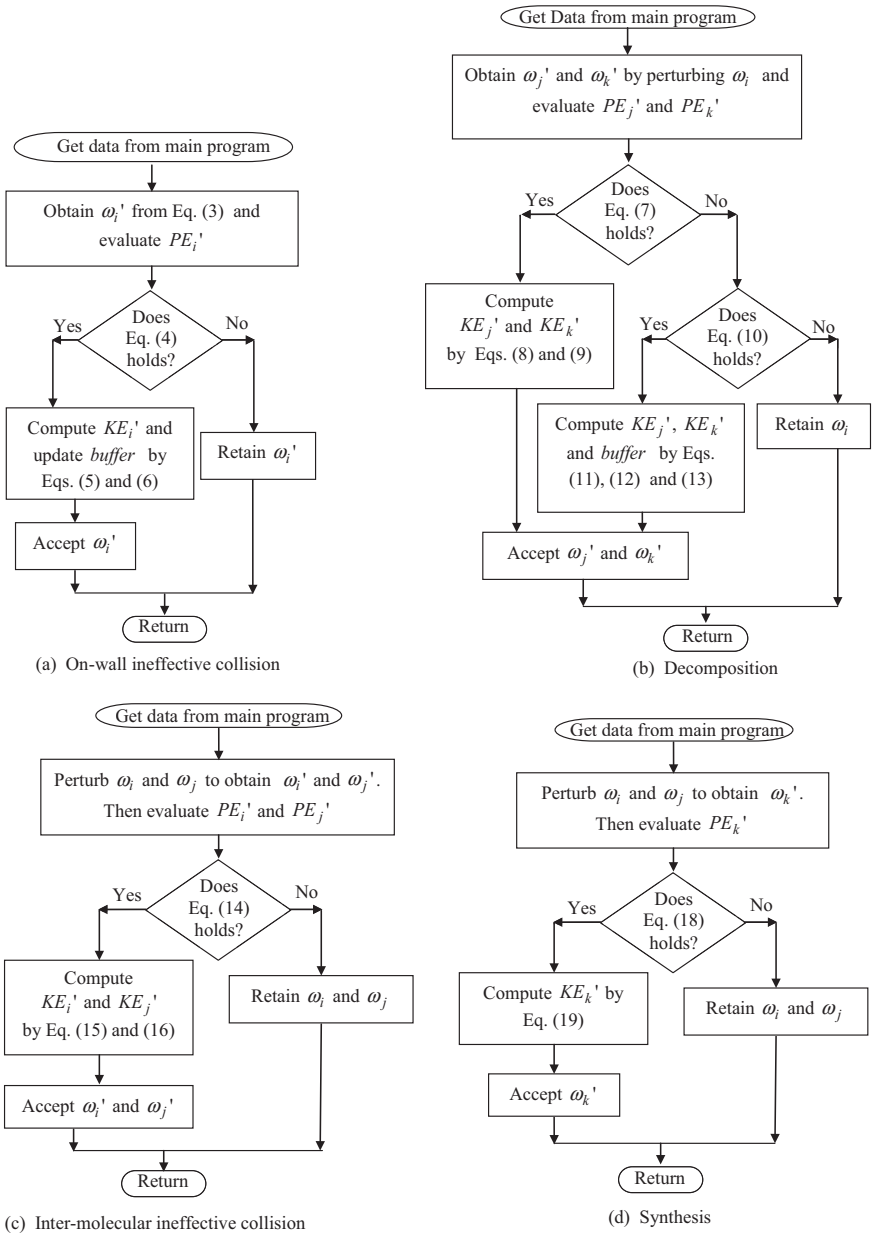

Figure 2 Subroutines of ACRO.

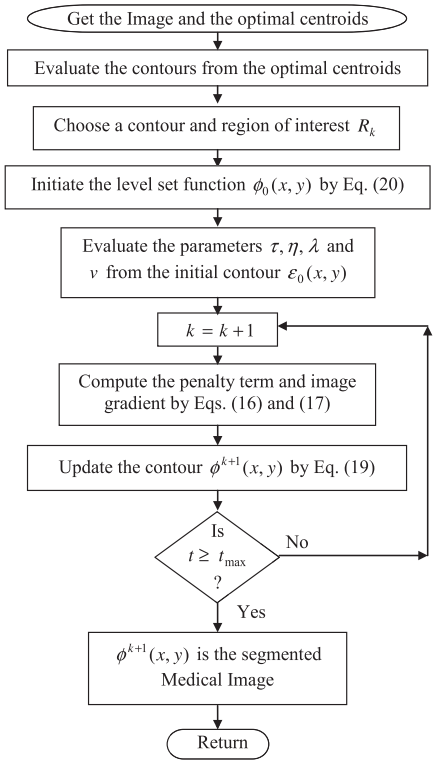

Figure 3 Subroutine - adaptive level set evolutions.

such as τ, β and γ, which are usually chosen by a trial and error process. An adaptive scheme for adjusting the parameters during evolution has been suggested in [15]. The PM also uses the adaptive adjustment of the parameters.

The level set evolution will be faster if the component of interest is large. In this case, the ratio of area to length of the initial level set function ϕ_0 will also be large and is set as the time step τ in the PM.

$$\tau = \frac{\int_l H(\phi_0)dxdy}{\int_l \delta(\phi_0)dxdy} \tag{29}$$

where $H(\phi_0)$ represents the Heaviside function and is defined as

$$H(\phi_0) = \begin{cases} 1, & \phi_0 \geqslant 0 \\ 0, & \phi_0 < 0 \end{cases} \tag{30}$$

The product of time step τ and penalty coefficient η should be less than 0.25 for stable evolution and hence the penalty coefficient is set as

$$\eta = 0.2/\tau \tag{31}$$

As the initial level set function ϕ_0 will represent approximated boundaries, the coefficient of the contour length for smoothness regulation λ is set as

$$\lambda = 0.1\tau \tag{32}$$

The balloon force v can be enhanced to pull or push the dynamic interface adaptively toward the object of interest as

$$v = 1 - 2R_k \tag{33}$$

The resulting balloon force $v \in [-1, 1]$ is a matrix with a variable pulling and pushing force at each image pixel, which makes the level set function be attracted toward the object of the interest regardless of its initial position.

The adaptive setting of parameters makes the level set evolution to move toward the genuine object. The level set function will automatically slow the evolution down and become dependent on the smoothing term, once the search approaches the final object.

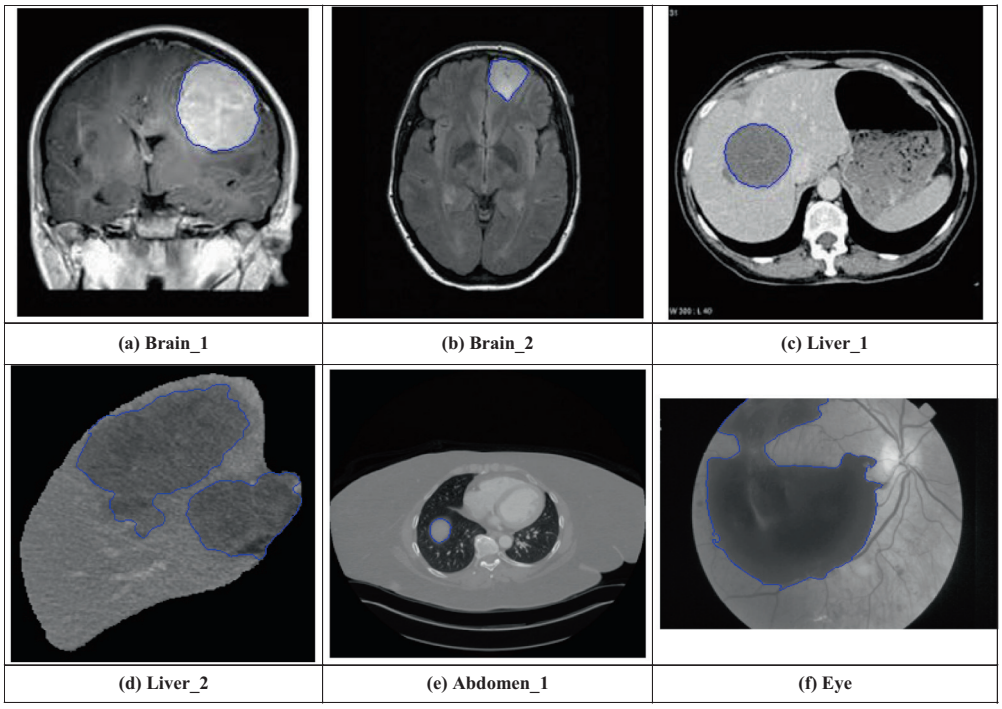

Figure 4 Medical images with ground truth marking.

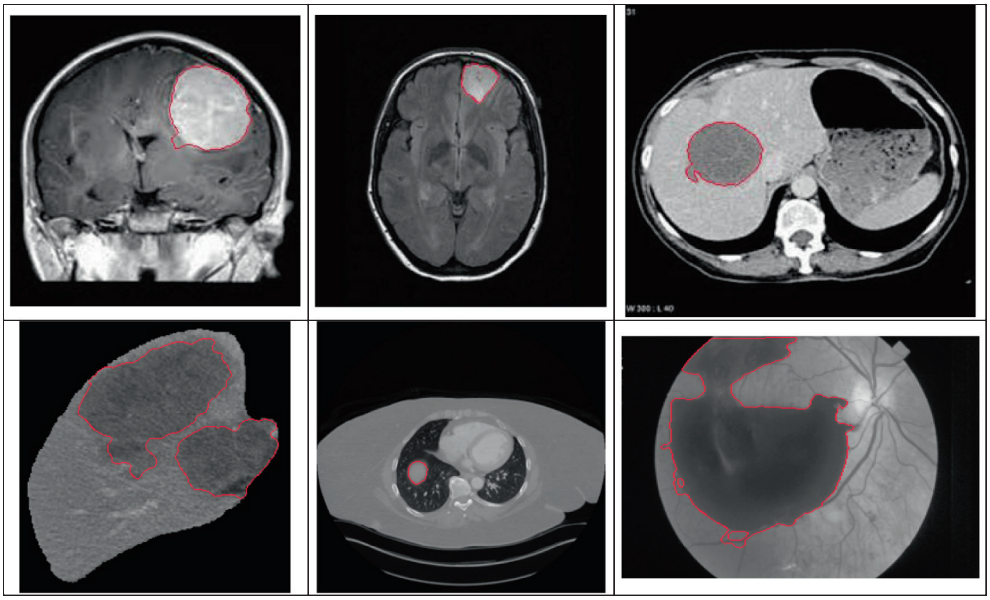

Figure 5 Results of PM.

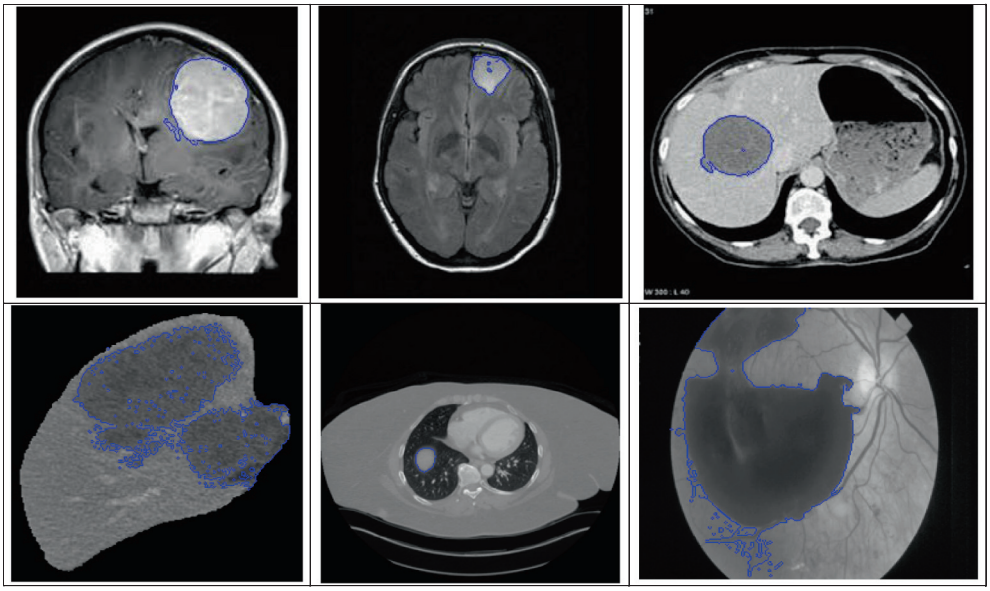

Figure 6 Results of TH.

4.3. Optimal segmentation process

The population containing molecules is initialized by random values within the respective decision variable limits for the given medical image. The ACRO search process is performed through chemical reactions involving the on-wall ineffective collisions, decomposition, inter-molecular ineffective collision and synthesis, after evaluating the *PE* values. The molecule with lowest PE is recorded and the iterative process is continued till convergence. The membership functions corresponding to the best molecule are the approximated contours. The counter of interest and the region of interest are chosen and fed to initiate level set function $\phi_0(x, y)$. The adaptive parameters are evaluated and the level set evolutions are performed till convergence. The contour at the end of convergence represents the segmented image of the given medical image. The flow of the segmentation process is explained through flowcharts of Figs. 1–3.

5. Results and discussions

The PM is applied on different types of medical images that include brain, lever, abdomen and eye images [34]. The brain, liver and abdomen images contain cancer, while the eye image is with sub-conjunctival hemorrhage. These images are shown in Fig. 4, which also includes the manually delineated cancer/hemorrhage region drawn by an expert. The manually delineated region is taken as the ground truth for studying the per-

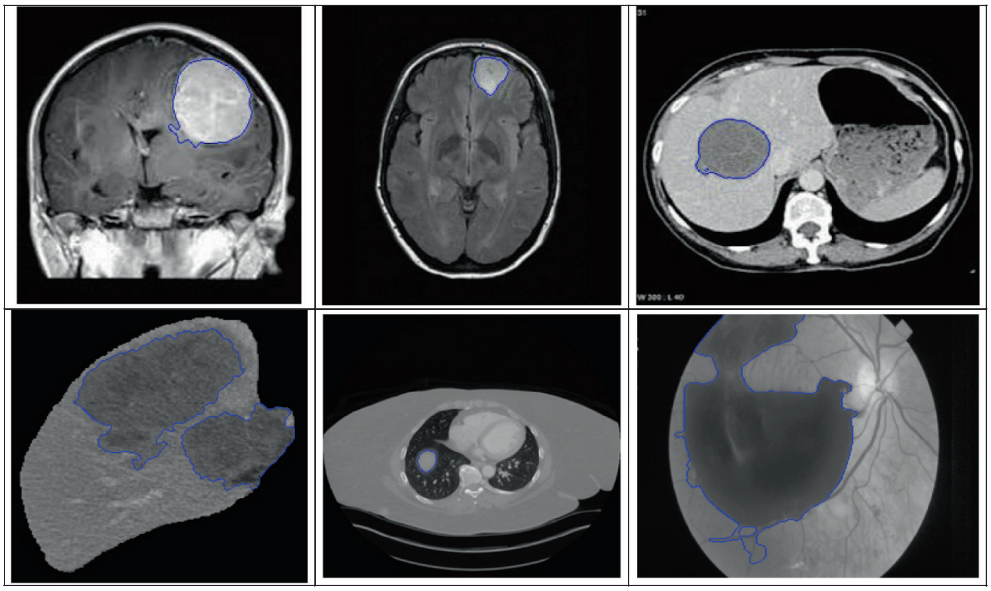

Figure 7 Results of KM.

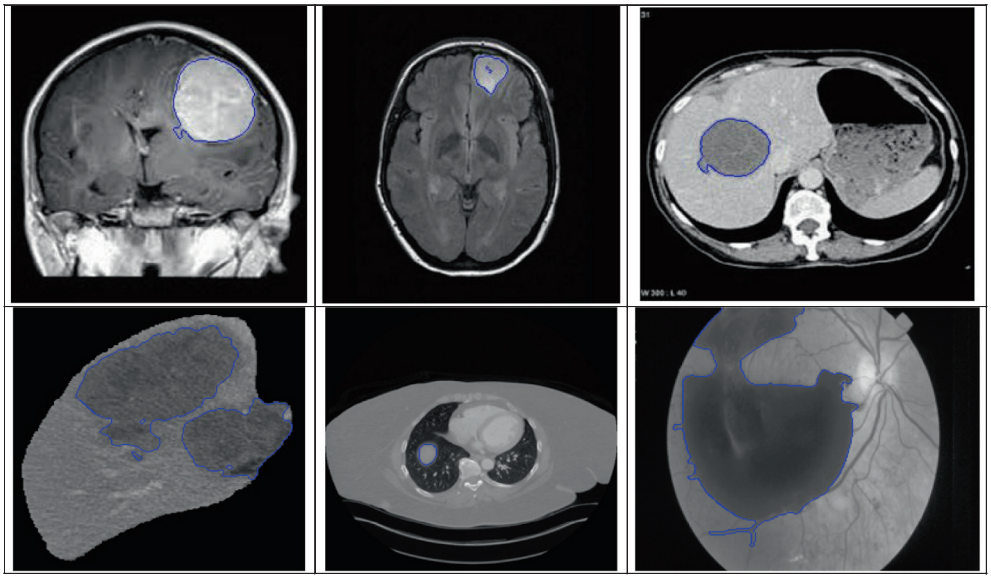

Figure 8 Results of FCM.

formances. The results of the PM are compared with those of the existing thresholding (TH) [11], K-means (KM) [18], fuzzy C-means (FCM) [21] and intuitionistic fuzzy C-means (IFCM) [22] methods. The segmented results of PM for all the medical images are presented in Fig. 5. The results of TH, KM, FCM and IFCM for the test images are shown in Figs. 6–9 respectively. The visual comparison of these results with those of the ground truth results clearly indicates that the PM is able to produce almost same results as that of ground truth images, while the results of existing methods deviate a bit from the ground truth images.

The performance of the proposed segmentation technique is quantitatively evaluated using four indices such as sensitivity, specificity, Jaccard index and Dice coefficients. Sensitivity represents percentage of cancer pixels properly included in segmentation results out of all the pixels in the results of segmentation. Specificity means percentage of cancer pixels properly excluded from the segmentation results out of all the pixels outside of ground truth. These indices are defined as follows:

$$\%SenInd = \left(\frac{TP}{TP + FN}\right) \times 100 \tag{34}$$

$$\%SpeInd = \left(\frac{TN}{TN + FP}\right) \times 100 \tag{35}$$

where True Positive (TP) denotes a pixel appearing in both manually segmented region and area detected by computerized method. True Negative (TN) represents a pixel absent in both manually segmented region and area detected by computerized method. False Positive (FP) means a pixel absent in manually

Please cite this article in press as: Asanambigai V, Sasikala J, Adaptive chemical reaction based spatial fuzzy clustering for level set segmentation of medical images, Ain Shams Eng J (2016), http://dx.doi.org/10.1016/j.asej.2016.08.003

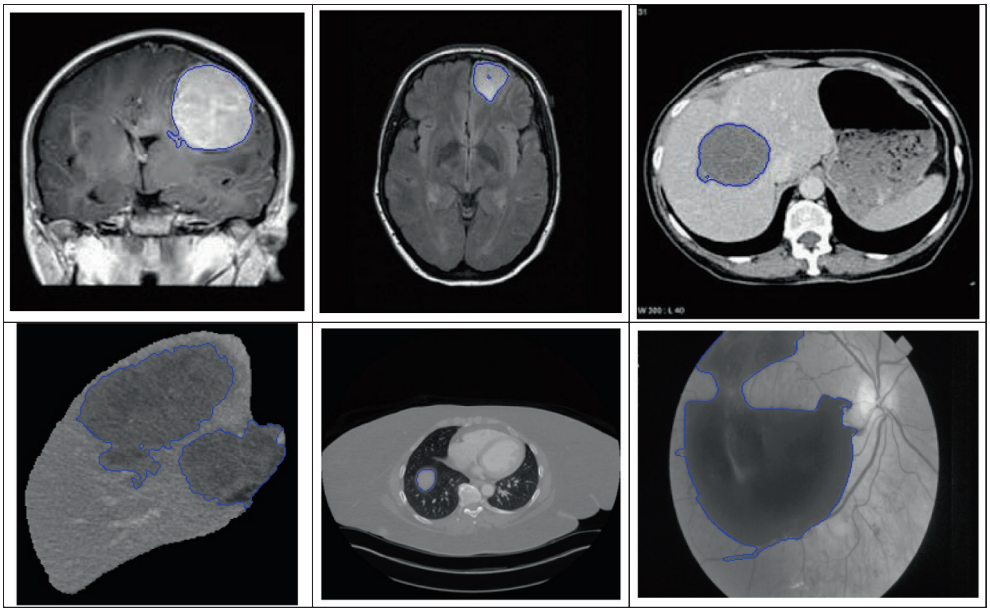

Figure 9 Results of IFCM.

Table 1 Comparison of performances.

Index	Image	PM	TH	KM	FCM	IFCM
%SenInd	Brain-1	84.56	78.42	79.95	83.72	84.21
	Brain-2	91.72	78.17	81.43	86.19	90.49
	Liver-1	85.03	82.53	83.17	84.66	84.16
	Liver-2	91.49	71.39	76.58	87.13	90.63
	Abdomen	90.43	84.26	84.89	89.07	90.17
	Eye	82.57	69.41	71.12	78.45	82.41
%SpeInd	Brain-1	92.16	83.83	87.78	91.12	91.89
	Brain-2	97.23	90.37	92.81	95.41	96.82
	Liver-1	93.67	86.56	87.53	89.18	92.22
	Liver-2	98.07	86.39	87.49	95.81	97.95
	Abdomen	96.36	87.13	88.07	94.28	96.11
	Eye	92.11	86.69	87.18	86.91	89.25
JacInd	Brain-1	0.909	0.827	0.846	0.879	0.891
	Brain-2	0.916	0.818	0.831	0.893	0.904
	Liver-1	0.874	0.819	0.823	0.849	0.861
	Liver-2	0.903	0.706	0.719	0.763	0.848
	Abdomen	0.896	0.803	0.823	0.846	0.864
	Eye	0.913	0.694	0.728	0.877	0.908
DiceCo	Brain-1	0.917	0.841	0.861	0.894	0.906
	Brain-2	0.923	0.826	0.839	0.901	0.912
	Liver-1	0.891	0.833	0.831	0.863	0.875
	Liver-2	0.910	0.732	0.731	0.771	0.879
	Abdomen	0.906	0.817	0.856	0.860	0.893
	Eye	0.921	0.724	0.741	0.893	0.916

segmented area, but it appears in the boarder detected by computerized method. False Negative (FN) indicates a pixel appearing in the manually segmented region boarder but it is absent from the boarder detected by computerized method [35].

Jaccard index is a statistical measure of similarity between the ground truth region and segmented region by the computerized method. It is defined as the cardinality of their intersection divided by the cardinality of the union:

$$JacInd = \frac{\Theta_{GT} \cap \Theta_{CM}}{\Theta_{GT} \cup \Theta_{CM}} \tag{36}$$

The Dice coefficient is defined as

$$DiceCo = 2 \times \frac{\Theta_{GT} \cap \Theta_{CM}}{\Theta_{GT} + \Theta_{CM}} \tag{37}$$

where Θ_{GT} represents manually segmented ground truth region and Θ_{CM} represents area detected by the computerized

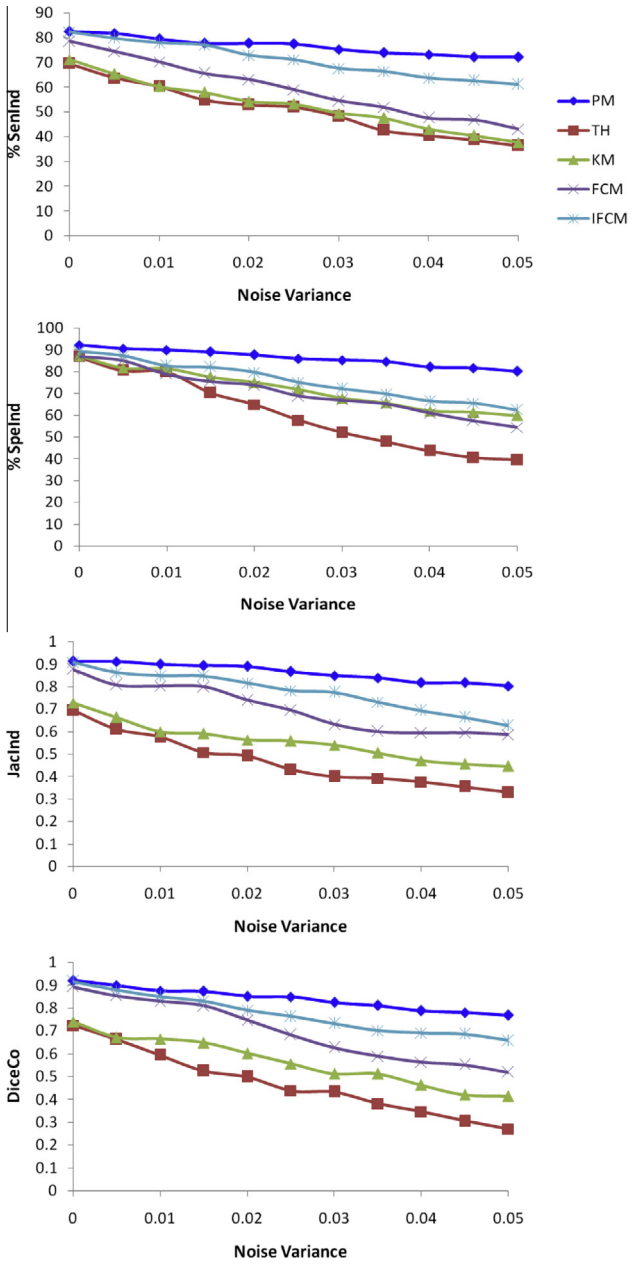

Figure 10 Performance indices at different noise levels for eye image.

method. These indices are calculated for the results of all the methods under study and given in Table 1. These values clearly indicate that the PM performs better in obtaining results that almost match the ground truth results.

In order to study the performance under noisy environment, the eye image is corrupted by different variances of Gaussian noise and processed by all the methods. The performance indices are calculated for all the results and graphically presented through Fig. 10. The decay of these indices of the PM is very small and nearer to noiseless case, while the variation of indices for other methods is much higher. It is very clear from these results that the PM is less affected by the increased noises compared to other methods, thereby establishing that the PM is robust. The above discussions clearly indicate that the PM outperforms the existing approaches and is suitable for segmentation of medical images, especially in noisy environments.

6. Conclusion

A new ACRO based fuzzy clustering method involving level set evolutions for segmenting the cancer and other unhealthy regions in medical images has been proposed. The adaptive mechanism helps to avoid local minima and the ACRO is able to provide the global best centroids considering spatial information. The level set evolutions facilitate the final segmentation for the chosen cluster. The various performance indices calculated for the PM as well for the existing methods of TH, KM, FCM and IFCM, clearly indicate the superiority of the PM even under noisy environment. Unlike other methods, the approach is able to process all kinds of medical images and helps the radiologist to analyze cancers and other unhealthy regions in various medical images.

References

[1] World health organization cancer fact sheets. <http://www.who.int/mediacentre/factsheets/fs297/en/index.html>.
[2] Sharma N, Aggarwal L. Automated medical image segmentation techniques. J Med Phys 2010;35:3–14.
[3] Lam AYS, Li VOK. Chemical-reaction-inspired metaheuristic for optimization. IEEE Trans Evol Comput 2010;14(3):381–99.
[4] Lam Albert YS, Li Victor OK, Yu James JQ. Real-coded chemical reaction optimization. IEEE Trans Evol Comput 2012;16(3):339–53.
[5] Bhattacharjee Kuntal, Bhattacharya Aniruddha, nee Dey Sunita Halder. Solution of economic emission load dispatch problems of power systems by real coded chemical reaction algorithm. Electr Power Energy Syst 2014;59:176–87.
[6] Xu J, Lam AYS, Li VOK. Chemical reaction optimization for task scheduling in grid computing. IEEE Trans Parallel Distrib Syst 2011;22(10):1624–31.
[7] Yu JJQ, Lam AYS, Li VOK. Evolutionary artificial neural network based on chemical reaction optimization. In: Proc IEEE CEC. p. 2083–90.
[8] Gonzalez RC, Woods RE. Digital image processing. New Jersey: Prentice Hall; 2007.
[9] Mostafa A, Elfattah MA, Fouad A, Hassanien AE, Hefny H. Wolf local thresholding approach for liver image segmentation in CT images. Adv Intell Syst Comput 2016;427:641–51.
[10] Baradez MO, McGuckinb CP, Forrazb N, Pettengell R, Hoppe A. Robust and automated unimodal histogram thresholding and potential applications. Pattern Recognit 2004;37(6):1131–48.
[11] Natarajan P, Krishnan N, Kenkre NS, Nancy S, Singh BP. Tumor detection using threshold operation in MR brain images. In: Proc IEEE Int Conf Comput Intell Comput Res. p. 1–4.
[12] Shih FY, Cheng S. Automatic seeded region growing for color image segmentation. Image Vis Comput 2005;23:877–86.
[13] Hojjatoleslami SA, Kittler J. Region growing: a new approach. IEEE Trans Image Process 1998;7(7):1079–84.
[14] Rouhi R, Jafari M. Classification of benign and malignant breast tumors based on hybrid level set segmentation. Expert Syst Appl 2016;46(C):45–59.
[15] Li Bing Nan, Chui Chee Kong, Chang Stephen, Ong SH. Integrating spatial fuzzy clustering with level set methods for automated medical image segmentation. Comput Biol Med 2011;41:1–10.
[16] Papamichail GP, Papamichail DP. The k-means range algorithm for personalized data clustering in e-Commerce. Eur J Oper Res 2007;177(3):1400–8.

[17] Clausi DA. K-means iterative fisher (KIF) unsupervised clustering algorithm applied to image texture segmentation. Pattern Recognit 2002;35(9):1959–72.
[18] Juang LH, Wu MN. MRI brain lesion image detection based on color-converted k-means clustering segmentation. Measurement 2010;43:941–9.
[19] Carvalho ATF. Fuzzy C-means clustering methods for symbolic interval data. Pattern Recognit Lett 2007;28(4):423–37.
[20] Chen SC, Zhang DQ. Robust image segmentation using FCM with spatial constraints based on new kernel-induced distance measure. IEEE Trans Syst, Man, Cybernetics, Part B: Cybernetics 2004;34(4):1907–16.
[21] Chuang KS, Tzeng AL, Chen S, Wu J, Chen TJ. Fuzzy c-means clustering with spatial information for image segmentation. Comput Med Imaging Graph 2006;30:9–15.
[22] Chaira T. A novel intuitionistic fuzzy C-means clustering algorithm and its application to medical images. Appl Soft Comput 2011;11:1711–7.
[23] Comaniciu D, Meer P. Mean shift: a robust approach toward feature space analysis. IEEE Trans Pattern Anal Mach Intell 2002;24(5):1–18.
[24] Omran MGH, Salman A, Engelbrecht AP. Dynamic clustering using particle swarm optimization with application in image segmentation. Pattern Anal Appl 2005;8(1):332–44.
[25] Ma M, Liang J, Guo M, Fan Y, Yin Y. SAR image segmentation based on artificial bee colony algorithm. Appl Soft Comput 2011;11(8):5205–14.
[26] Cinsdikici MG, Aydin DA. Detection of blood vessels in ophthalmoscope images using MF/ant (matched filter/ant colony) algorithm. Comput Methods Prog Biomed 2009;96(2):85–95.
[27] Aydın D, Ugur A. Extraction of flower regions in color images using ant colony optimization. Proc Comput Sci 2011;3(1):530–6.
[28] Akay B. A study on particle swarm optimization and artificial bee colony algorithms for multilevel thresholding. Appl Soft Comput 2013;13(1):3066–91.
[29] Kumar M, Rawat TK. Optimal fractional delay-IIR filter design using cuckoo search algorithm. ISA Trans 2015;59:39–54.
[30] Kumar M, Rawat TK. Optimal design of FIR fractional order differentiator using cuckoo search algorithm. Expert Syst. Appl. 2015;42(7):3433–49.
[31] Aggarwal A, Rawat TK, Kumar M, Upadhyay DK. Design of optimal band-stop FIR filter using L1-norm based RCGA. Ain Shams Eng J 2016. http://dx.doi.org/10.1016/j.asej.2015.11.022.
[32] Saha S, Alok AK, Ekbal A. Brain image segmentation using semi-supervised clustering. Expert Syst Appl 2016;52(C):50–63.
[33] Gao Hao, Pun Chi-Man, Kwong Sam. An efficient image segmentation method based on a hybrid particle swarm algorithm with learning strategy. Inf Sci 2016. http://dx.doi.org/10.1016/j.ins.2016.07.017.
[34] Cancer Imaging Archive, http://www.cancerimagingarchive.net.
[35] Metz C. Basic principles of ROC analysis. Semin Nucl Med 1978;8:283–98.

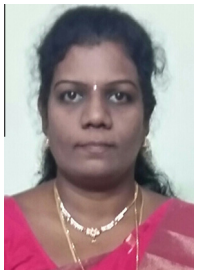

Mrs. V. Asanambigai received the B.E. and M. E. Degrees in Computer Science and Engineering from Annamalai University, India, in 2002 and 2005 respectively, and is working toward her Ph.D. degree. She has been working as an Assistant Professor in the Department of Computer Science and Engineering, Annamalai University, Tamil Nadu, India, since 2007. Her research interests are in the area of evolutionary algorithms and image processing.

Dr. J. Sasikala received the B.E. Degree in Electronics and Communication Engineering from Madras University, India, in 1993, and the M.E. and Ph.D. degrees in Computer Science and Engineering from Annamalai University, India, in 2005 and 2011 respectively. She has been working as an Assistant Professor in the Department of Computer Science and Engineering, Annamalai University, Tamil Nadu, India, since 1999. Her research interests are in the area of optimization, evolutionary algorithms and image processing.

Please cite this article in press as: Asanambigai V, Sasikala J, Adaptive chemical reaction based spatial fuzzy clustering for level set segmentation of medical images, Ain Shams Eng J (2016), http://dx.doi.org/10.1016/j.asej.2016.08.003